La mer 43 : 89-96, 2005
Société franco-japonaise d'océanographie, Tokyo

A westward propagation signal in the sea ice concentration in the Indian sector of the Southern Ocean

Xuhui XIE*, Hideki NAGASHIMA, and Masao NEMOTO

Abstract : From longitude-time plots for Sea Ice Concentration (SIC) anomalies along 63.71 °S in the period 1979 to 1999, a wave-like pattern is found to propagate westward from 60°E to 140°E. This pattern fluctuates with a period of nearly 5 years and propagates at a speed of approximately 3.3 cm/s. Such characteristics differ from those of the Antarctic Circumpolar Wave (ACW), the signal for which repeats every 4-5 years, and which propagates eastward around Antarctica with an average speed of about 8 cm/s. A 48-month time-lagged extended empirical orthogonal function (EEOF) analysis of SIC anomalies shows that SIC variability with interannual time scales is negatively coupled to SST fluctuations, and the SIC anomalies propagates eastward in the Pacific and Atlantic oceans. In the Indian Ocean from 60°E to 140 °E, however, this analysis cannot identify such a negative correlation.

Keywords : *sea ice concentration, EEOF, EOF, westward propagation*

1. Introduction

The Sea Ice Concentration (SIC) in the Southern Ocean is considered to play an important role in the state and variability of both regional and global climates through the action of thermodynamic and dynamic processes and feedback mechanisms.

WHITE and PETERSON (1996) have reported that an interannual oscillation with a period of 3–4 years dominates in Sea Level Pressure (SLP), sea surface temperature (SST), meridional wind stress, and Sea Ice Extent (SIE) anomalies in the Southern Ocean. This fluctuation is named the Antarctic Circumpolar Wave (ACW). The signal repeats itself every 4–5 years and propagates eastward around Antarctica with an average velocity of about 8 cm/s in a phase-locked manner. The eastward propagation of the ACW was also found by JACOBS and MITCHELL (1996), who observed coherent variations in sea surface height, SST, and atmospheric pressure. Those authors showed that the eastward-propagating ACW has a period of about 4 years and a wavelength of 180 degrees in longitude.

WHITE and PETERSON (1996) have suggested a tele-connection of ACW with the El Niño-Southern Oscillation (ENSO) phenomenon. Their model simulations of the ACW demonstrate that there must be a coupling between ocean and atmosphere for this phenomenon to exist. QIU and JIN (1997) Showed that the mechanism of the ACW is based on a local ocean-atmosphere interaction.

In addition to elucidating the ACW's variability many studies have suggested that the Antarctic sea ice fields co-vary with the ENSO phenomenon in the tropical Pacific (CHIU, 1983; CARLETON, 1989; SIMMONDS and JACKA, 1995; WHITE and PETERSON, 1996; YUAN *et al.*, 1996; SMITH *et al.*, 1996; LEDLEY and HUANG, 1997; CARLETON *et al.*, 1998; YUAN and MARTINSON 2000, 2001; HARANGOZO, 2000; KWOK and COMISO, 2002; MARTINSON and IANNUZZI, 2003; YUAN, 2004). Recently, YUAN and MARTINSON (2000) found that an out-of-phase relationship between SIC and SST anomalies in the South Pacific and South Atlantic persists three to

*Department of Ocean Sciences, Tokyo University of Marine Science and Technology, Konan 4-5-7, Minatoku, Tokyo 108-8477, Japan
Telephone: 03-5463-0465 Fax: 03-5463-0378
E-mail: xifui2003@yahoo.co.jp

four seasons after being triggered by the ENSO forcing. This relationship is called the Antarctic dipole (ADP).

From the analysis of SIC variability inside the ice pack, GLOERSEN and WHITE (2001) found evidence to support that the thermal inertia associated with the SST provides the most dominant factor influencing the amount of sea ice that forms each winter around Antarctica. They concluded that the memory of the ACW in the sea ice pack is carried from one austral winter to the next by the neighboring water temperatures, since the sea ice pack retreats nearly to Antarctica in austral summer.

As mentioned above, the ACW is now one of the most notable phenomena around Antarctica. VENEGAS (2003), however, pointed out that there is another signal in the SST fluctuations, propagating westward in the western Indian Ocean between 45° E and 90° E. As SST data are not available near Antarctica because of sea ice, especially in austral winter, the SIC analysis will help clarify the existence of the westward-propagating signal near and around Antarctica. Thus, we focus on SIC variability near Antarctica especially in the Indian sector and investigate both its interannual fluctuation characteristics and the relationship between the spatial variability in the Antarctic SIC and global SST.

In this paper, we carry out an empirical orthogonal function analysis of SIC anomalies. In section 3, we show that the signal of the ACW is unclear near the coastal area in the Indian sector, although the general characteristics of SIC fluctuations are similar to those in SIE, SLP, and so on. Next, in section 4, a westward-propagating signal is shown from the longitude-time analysis of SIC anomalies along 63.71° S. A discussion and concluding remarks are given in sections 5 and 6, respectively.

2. Data collection and methodology

Two data sets are used in this study: (1) the monthly mean SIC; the areal fraction covered by sea ice is obtained irrespective of ice type, and the ratio describing the density of ice is derived from grid brightness temperatures, ranging from 0 to 100%. The data set spans 21 years from 1979 to 1999 and was provided by the National Snow and Ice Data Center (NSIDC). These data are derived from SSMR and SSM/I satellite passive microwave observations with a grid resolution of 25 km. (2) The monthly optimum interpolation (OI) of SST data spans an 18-year period from 1982 to 1999 and was provided by the National Centers for Environmental Prediction (NCEP). A set of 1° × 1° grid data was derived from a combination of *in situ* and satellite radiometer measurements.

These data sets are processed to determine the mean annual cycle and to compute the monthly average over the record length. Time series of monthly anomalies in each grid were determined by the difference relative to the monthly mean values for the applicable record length. Such procedures result in the removal of the average seasonal cycle.

To suppress further seasonal and possible biennial signals, and also to remove long-term trends, the time series were band-passed with a filter having a 3–7 year admittance window. A time-longitude diagram is then created.

3. Empirical orthogonal function (EOF) analysis of SIC anomalies

In the present study, the sea ice region is defined by a group of grids in which the SIC is greater than 15% at least once a month during the 21-year period.

The SIC anomalies are rearranged into an N × P matrix, where the number of samples N is the time series of 252 months from 1979 to 1999, and the parameter P (=4678) is taken as the number of grids describing the sea ice region. From this data matrix, a 4678-square spatial covariance matrix is calculated.

The EOF leading mode eigenvector has 7.6% of the total SIC variance (shown in Fig.1a). From the power spectral analysis (Fast Fourier Transform) of the leading EOF score drawn in Fig. 1b, it is found that there is a significant peak in the spectral energy at a period of 3.5 years (0.0238 cycles mon^{-1}), as shown in Fig. 1c. This analysis revealed the most important patterns of spatially and temporally coherent variability in SIC anomalies.

Many studies have suggested a mode-3 wave in the Southern Ocean. For example, COMISO (2000) indicated that the Antarctic sea ice cover

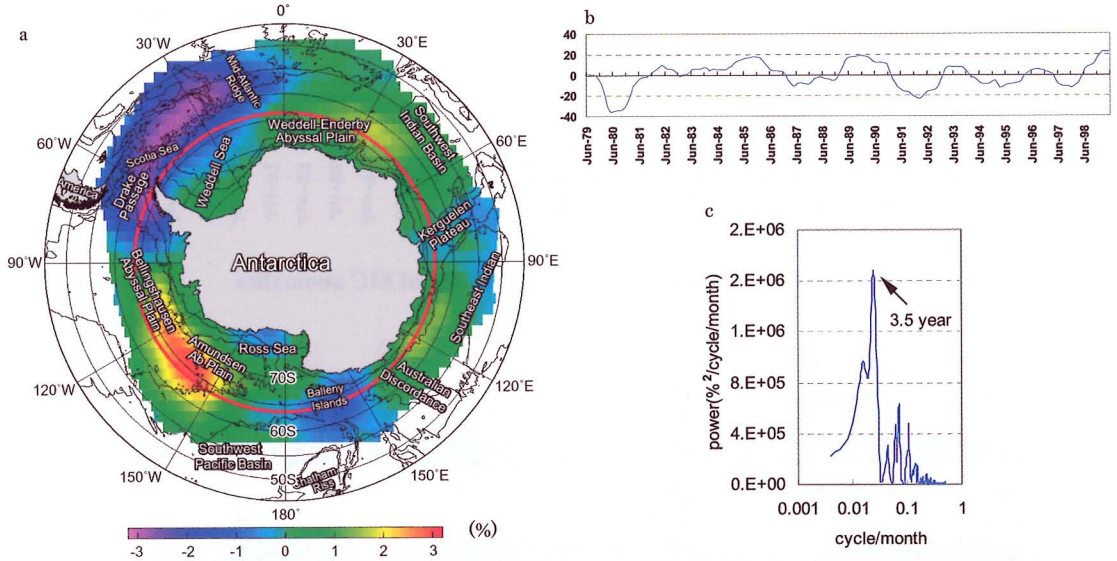

Fig. 1a). Leading EOF mode eigenvector of SIC (%) anomalies contains 7.6% of the total SIC variance from Jan 1979 to Dec 1999. High amplitudes occur in the Bellingshausen Abyssal Plain, Drake Passage, and Scotia Seas, indicating positive SIC anomalies and negative SIC anomalies, respectively. The leading EOF mode eigenvector shows a spatial pattern of wave number 3; the largest wave spans longitudes between 160°W and 10°E, the second largest wave was detected in the region from 90°E to 180°, and the third largest wave, from 10°E to 90°E, was very weak. The color bar ranges from —25 to 25 (%). The red circle is the longitude of the 63.71°S.

b) Temporal variation in the score of the leading EOF mode of SIC anomalies in the Southern Ocean.

c) Spectra of the leading EOF score of SIC anomalies obtained during the 21-year period from 1979 to 1999 show a significant peak in the period of about 3.5 years.

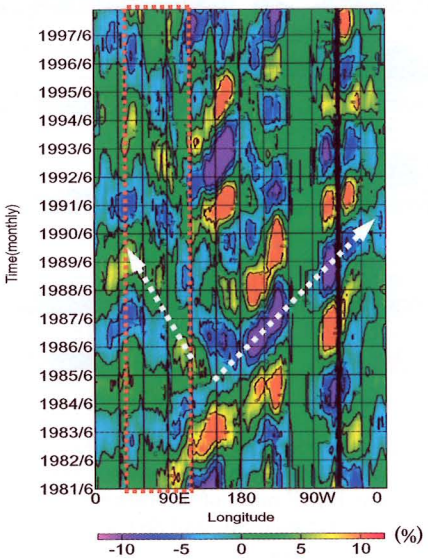

Fig. 2. Time-longitude diagrams of SIC (%) anomalies after passing through a 3–7 year band-pass filter. In the Pacific and Atlantic oceans (from 140°E to 60°E), an eastward ACW-type propagation occurs. Conversely, that in the Indian Ocean (from 60°E to 140°E) propagates westward. The color bar ranges from −12 to 12 (%).

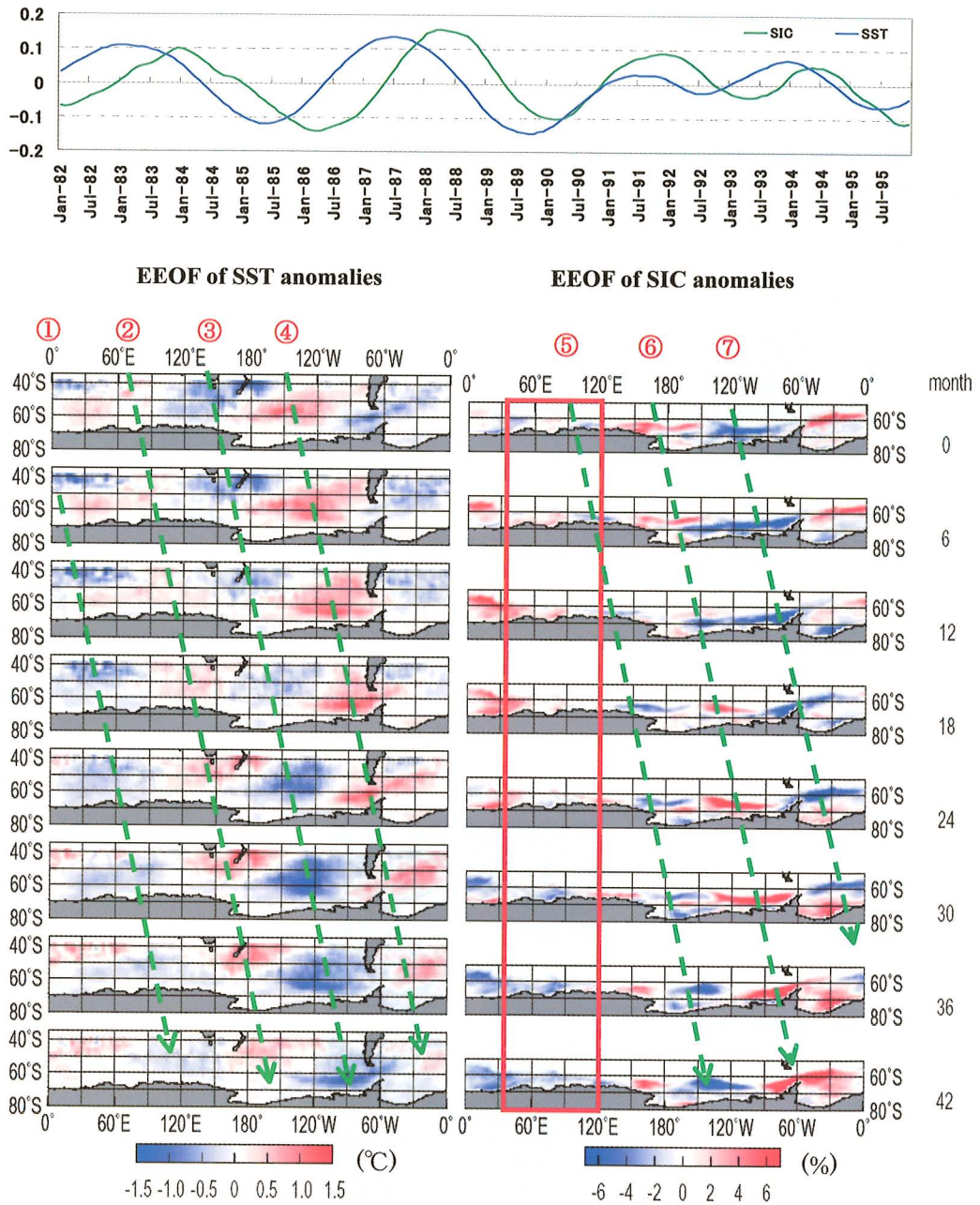

Fig. 3. Top panel: Temporal variation in the scores of the leading EEOF mode of SIC and SST anomalies in the Southern Ocean after passing through a 3–7 year band-pass filter. The cross-correlation is 0.80. Bottom panel: Lag sequences of the dominant EEOF mode of interannual SIC (%) and SST (°C) anomalies. Broken lines show a clear negative correlation between SIC and SST anomalies; they all propagate eastward in the Pacific and Atlantic oceans. In the Indian Ocean, however, there is not always a negative correlation between SIC and SST anomalies. In months 6–18, positive SST anomalies dominate in the Indian sectors, and positive SIC anomalies also appear in this region. In months 30–42, a negative SST and SIC dominate in the region. The color bar ranges from −1.5 to 1.5 (°C), and for SIC anomalies the color bar ranges from −7 to 7 (%).

consists predominantly of mode-3 waves. CONNOLLEY (1997) analyzed SLP anomalies, and Hans et al. (1999) analyzed SLP and the curl of wind stress. In both of those studies, the authors found a similar pattern of the mode-3 wave. In those studies, a spatial pattern with a wave number 3 is also found in the Southern Ocean. The largest wave is found to span from 160° W to 10° E. Positive/negative SIC anomalies occur in the Bellingshausen Abyssal Plain/Drake Passage and in the Scotia Sea. The second largest wave is detected in the region from 90° E to 180°, and the third largest wave, between 10° E and 90° E, is very weak.

4. Propagation characteristics of the westward wave-like signal observed in SIC records in the Indian sector of the Southern Ocean

As described in section 3, the EOF first mode of SIC anomalies shows three waves around Antarctica, the second largest of which is in the Indian sector. The peak and trough of the wave are found around 64° S. Since the Antarctic coast extends further north in this sector and the Antarctic Circumpolar Current (ACC) is a little far from this latitude, the propagation characteristics are probably different from those in other sectors.

Thus, we plot SIC anomalies along 63.71° S near 64° S on a time-longitude diagram, because this latitude is located almost at the center of a 25×25 km cell. The horizontal resolution of the data analyzed is 1° in longitude. The results are illustrated in Fig. 2. One question is whether or not an ACW-type signal is apparent in the SIC anomalies. Actually, the SIC anomalies depicted in the diagram reveal clear eastward propagation signals in the Pacific and Atlantic oceans. In contrast, a westward propagation is quite apparent in the Indian Ocean between 60° E and 140° E. This propagation is in contrast to the more familiar ACW type.

The SIC anomalies in the Pacific and Atlantic oceans appear to propagate eastward with a period of 3–5 years. It takes 7–9 years to circle Antarctica at an average propagation velocity of about 6–8 cm/s. On the other hand, the SIC anomalies in the Indian Ocean propagate westward over a slightly longer period, nearly 5 years, and their velocity is about 3.3 cm/s, which is slower than that of the eastward propagation observed.

Similar westward-propagating signals are found around 60° S and 65° S, but the signal around 64° S is clearer than the others. Note that the time-longitude analysis for SST anomalies around 45° S, 50° S, 55° S, and 60° S suggests that the eastward-propagating signal is not so clear (not shown here) in the Indian sector around 60° S.

As mentioned above, the propagation characteristics in the Pacific and Atlantic oceans are similar to those for the ACW described by WHITE and PETERSON (1996). In the Indian Ocean, however, the SIC anomalies appears to propagate to the opposite direction and with a slower velocity. One of the reasons for this difference must be the topography of the Indian Ocean. As shown in Fig. 1a, the Kerguelen Plateau and the Balleny Islands obstruct the eastward propagation of the ACC near the coast. Another reason is probably the existence of a cyclonic gyre of wind and current systems at high latitudes in the Indian sector of the Southern Ocean.

5. Discussion

As described above, the EOF analysis shows that the SIC anomalies propagate eastward in general. However, the time-longitude diagram along 63.71° S indicates a signal of westward propagation in the Indian Ocean. Thus, we discuss the time-space variability of SIC anomalies based on the EEOF analysis. The EEOF method has shown some promise for improving our understanding of the nature of the dominant patterns for coherent variability in space and time.

Here we apply EEOF to SST and SIC anomalies in order to clarify the relationship between them, and also to identify whether or not the westward propagation of the SIC anomalies is related to the SST anomalies in the Indian Ocean.

In Fig. 3, we show the results of the EEOF analysis for the SIC and SST anomalies. The scores of the leading EEOF mode of the SIC and SST anomalies with a 3–7 year band-pass filter have a cross-correlation of 0.80 (Fig. 3, top).

We identify the ACW propagation by EEOF analysis. SST anomalies (left panel in Fig. 3) slowly propagate eastward with the variability of interannual time scales. As shown by broken line 4, well-developed positive SST anomalies in the South Pacific extend in a zonal direction in months 0–6. Then, in months 12–18, the warm SST anomalies move slowly toward the east and ran into the Drake Passage around 70° W, causing large negative SIC anomalies in this region as shown by the broken line 7. In months 24-36, well-developed positive SIC anomalies in the Weddell Sea around 40° W prevent the eastern propagation of positive SST anomalies. The SST anomalies then become weaker and move to the east of the Atlantic and to the Indian Oceans in months 36–42, and the warm SST anomalies in this region move to a lower latitude. As a result, the SST anomalies slowly move eastward, traversing more than half of the Southern Ocean from 150° E to 90° E during a 42-month period. It is shown that SST anomalies fluctuate with a 3.5-year quasi-periodicity in the Southern Ocean. We also identify the eastward propagation of the SST anomalies shown by broken lines 1–3. WHITE and CHEN (2002) also indicated that an ACW with a 3–4 year period propagates eastward around the Southern Ocean, covaries with SST and SLP anomalies, and consists of two wavelengths circling most of the global ocean along the mid-latitude storm track near 40° S.

The propagation of positive SST anomalies shown by broken lines 2 and 4 corresponds to the propagation of negative SIC anomalies shown by broken lines 5 and 7, although they all propagate toward the east with time. In addition, the negative propagation of SST anomalies shown by broken line 3 corresponds to the positive propagation of SIC anomalies shown by broken line 6. Accordingly, a clear negative correlation between the SIC and SST anomalies over most of the Pacific sectors and the Atlantic sector of the Southern Ocean is suggested, and both the SST and SIC anomalies propagate eastward. In the Indian Ocean, however, there is not always a negative correlation between these two anomalies, although we can find eastward propagation in the SST but not in the SIC anomalies. In months 6–18, positive SST anomalies dominate in the Indian sectors, and positive SIC anomalies also appear in this region. In months 30–42, negative SST and SIC dominate in the region. Thus, the EEOF analyses show that there is not a strong negative correlation between SST and SIC anomalies in this region.

The ACW was observed to follow the mid-latitude storm track in the eastern Atlantic, Indian, and western Pacific sectors of the Southern Ocean between 30° S and 45° S (WHITE and CHEN, 2002). In addition, the ACW is the dominant climate signal in monthly SST, SLP, and SIE in the Southern Ocean (VENEGAS, 2003; WHITE, 2004; POTTIER *et al.* 2004). In the present study, however, westward propagation of SIC anomalies is implied in the Indian sector.

6. Concluding remarks

A brief summary of the sea ice variability in the Southern Ocean described in this paper is as follows.

Interannual oscillations with periods of about 3–5 years were found to characterize the SIC variability in the Southern Ocean. The SIC anomalies fluctuate with a peak of 3.5-year quasi-periodicity and with a spatial pattern of wave number 3. The largest wave appeared in the Pacific and Atlantic oceans. The second largest wave was detected in the region of the Indian Ocean. The third largest wave, from 90° E to 180°, was very weak.

We focused on the Indian sector and found that SIC anomalies propagate westward in the Indian Ocean. The anomalies fluctuate with a period of approximately 5 years and propagate at a speed of 3.3 cm/s. This is a little longer and slower than the ACW, which propagates eastward in the Pacific and Atlantic oceans.

EEOF analysis revealed a clear negative correlation between SIC and SST anomalies over most Pacific sector and the Atlantic sector of the Southern Ocean. In the Indian Ocean, however, there is rather a positive correlation between SIC and SST anomalies. We can find eastward propagations in SST anomalies, which are the characteristics of ACW, in all of the Southern Ocean, but we cannot find eastward propagation in SIC anomalies in the Indian sectors.

The westward propagation of the SIC anomalies shows little association with the SST in the Indian sector. We suggest that this is probably affected by topography and is associated with currents moving westward along the coast. The Kerguelen Plateau and the Balleny Islands obstructed the eastward propagation of the covarying ACC, resulting in a westward current. Similarly, obstacles to the westward propagation of this near-coastal current are likely to result in a similar augmentation of the ACC. These findings suggest that the westward propagation of the SIC anomalies is closely related to the westward current, which is generated by extensive gyres in the basins. Further studies on propagation characteristics in the Southern Ocean should focus on whether or not westward circumpolar propagation occurs inside the ACW near the continental Antarctic coast.

Acknowledgment

We are grateful to Dr. S. SUGIHARA, Dr. J.F. ZHAO, and Mr. Y. NARUMI of the Tokyo University of Marine Science and Technology for their fruitful and useful discussions with us.

References

CARLETON, A. M. (1989): Antarctic sea-ice relationships with indices of the atmospheric circulation of the Southern Hemisphere. Clim. Dyn., **3**, 207–220.

CARLETON, A. M., G. JOHN, and R. WELSCH (1998): Interannual variations and regionality of Antarctic sea-ice-temperature associations. Ann. Glac., **27**, 403–408.

CHIU, L. S. (1983): Antarctic sea ice variations 1973-1980. *In* Variations in the global water budget, Street-Perrott, F.A., M. Beran, and R. Ratcliffe, (eds.), Dordrecht: Reidel, 301–311.

COMISO, J. C. (2000): Variability and trends in Antarctic surface temperatures from in situ and satellite infrared measurements. J. Clim., **13** (**10**), 1674–1696.

CONNOLLEY, W. M. (1997): Variability in annual mean circulation in southern high latitudes. Clim. Dyn., **13**, 745–756.

GLOERSEN, P. and W. B. WHITE (2001): Reestablishing the circumpolar wave in sea ice around Antarctica from one winter to the next. J. Geophys. Res., **106**, 4391–4396.

HANS, B., S. ANDREAS and J. K. GERBRAND (1999): Interannual variability in the Southern Ocean from an ocean model forced by European Center for Medium-Range Weather Forecasts reanalysis fluxes. J. Geophys. Res., **104** (**13**), 317–13, 331.

HARANGOZO, S. A. (2000): A search for ENSO teleconnections in the west Antarctic Peninsula climate in austral winter. Int. J. Clim., **20**, 663–678.

JACOBS, G. A. and J. L. MITCHELL (1996): Ocean circulation variations associated with the Antarctic circumpolar wave. Geophys. Res. Lett., **23**, 2947–2950.

KWOK, R. and J. C. COMISO (2002): Southern Ocean climate and sea ice anomalies associated with the Southern Oscillation. J. Clim., **15**, 487–501.

LEDLEY, T. S. and Z. HUANG (1997): A possible ENSO signal in the Ross Sea. Geophys. Res. Lett., **24**, 3253–3256.

MARTINSON, D. G. and R. A. IANNUZZI (2003): Spatial/temporal patterns in Weddell gyre characteristics and their relationship to global climate. J. Geophys. Res., **108**, doi: 1029/2000JC000538.

POTTIER, C., J. P. CÉRON, J. SUDRE, I. DADOU, S. BELAMARI, and V. GARCON (2004): Dominant propagating signals in sea level anomalies in the Southern Ocean. Geophys. Res. Lett., **31**, L11305, doi: 10.1029/2004GL019565.

QIU, B. and F. F. JIN (1997): Antarctic circumpolar waves: An indication of ocean-atmosphere coupling in the extratropics. Geophys. Res. Lett., **24**, 2585–2588.

SIMMONDS, I. and T. H. JACKA (1995): Relationships between the interannual variability of Antarctic sea ice and the Southern Oscillation. J. Clim., **8**, 637–647.

SMITH, R. C., S. E. STAMMERJOHN, and K. S. BAKER (1996): Surface air temperature variations in the western Antarctic Peninsula region. Antarctic Research Series, **70**, 105–121.

VENEGAS, S. A. (2003): The Antarctic Circumpolar Wave: A combination of two signals? J. Clim., **16** (**15**) , 2509-2525.

WHITE, W. B. (2004): Comments on "Synchronous variability in the Southern Hemisphere atmosphere, sea ice, and ocean resulting from the annular mode". J. Clim., **17**, 2249–2254.

WHITE, W. B. and R. PETERSON (1996): An Antarctic circumpolar wave in surface pressure, wind, temperature, and sea ice extent. Nature, **380**, 699–702.

WHITE, W. B. and S. C. CHEN (2002): Thermodynamic mechanisms responsible for the troposphere response to SST anomalies in the Antarctic circumpolar wave. J. Clim., 15, 2577–2596.

YUAN, X. (2004): ENSO-related impacts on Antarctic sea ice: a synthesis of phenomenon and mechanisms. Antarctic Science, **16** (4), 415–425.

YUAN, X., M. A. CANE, and D. G. MARTINSON (1996): Climate variation - cycling around the South Pole. Nature, **380**, 673–674.

YUAN, X. and D. G. MARTINSON (2000): Antarctic sea ice extent variability and its global connectivity. J. Clim., **13**, 1697–1717.

YUAN, X. and D. G. MARTINSON (2001): The Antarctic dipole and its predictability. Geophys. Res. Lett., **28**, 3609–3612.

Received: October 25, 2005
Accepted: December 5, 2005